

Extensional arc setting and ages of Middle Jurassic eolianites, Cowhole Mountains (eastern Mojave Desert block, California)

Cathy J. Busby

*Department of Geological Sciences and Institute for Crustal Studies, University of California,
Santa Barbara, California 93106, USA*

Elizabeth R. Schermer

Department of Geology, Western Washington University, Bellingham, Washington, USA

James M. Mattinson

*Department of Geological Sciences and Institute for Crustal Studies, University of California,
Santa Barbara, California 93106, USA*

ABSTRACT

Mesozoic strata in the Cowhole Mountains, eastern Mojave block California, include 200–800 m of eolian quartz arenite (Aztec Sandstone) overlain by more than 575 m of silicic ignimbrites, lava flows, and minor sedimentary rocks (Cowhole volcanics). U-Pb zircon geochronologic data on a crystal-rich dacite lava flow in the Aztec Sandstone indicate that the sandstone is Middle Jurassic and is therefore age equivalent to backarc eolianites of the Temple Cap and Carmel Formations, not the Lower Jurassic Navajo Formation as previously assumed. Our U-Pb zircon data on two ignimbrites of the Cowhole volcanics indicate that they are the same age, within error, as the lava flow in the Aztec Sandstone at 170 ± 3 Ma. New structural and stratigraphic data, together with published data, indicate syndepositional normal faulting and deposition of landslide blocks throughout deposition of this section. These results are consistent with our previous volcanologic studies in Middle Jurassic rocks of southern Arizona, southeastern California, and the central Mojave block, which document ignimbrite eruptions from calderas contemporaneous with deposition of craton-derived eolian sands, in extensional or transtensional intra-arc basins.

INTRODUCTION

The Triassic–early Middle Jurassic continental arc of California, Arizona, and western Nevada has been postulated to have occupied a more-or-less-continuous graben-type depression, more than 1000 km long, similar to the setting of the modern extensional arc of Central America (Busby-Spera, 1988; Busby-Spera et al., 1990a). This graben-type depression apparently acted as a long-lived (>40 m.y.) trap for Lower and Middle Jurassic craton-derived quartz arenites (Busby-Spera, 1988; Riggs et al., 1993; Fackler-Adams et al., 1997). Obser-

vations remain too scattered to determine the degree of lateral continuity of the postulated graben-type depression, largely because late Mesozoic shortening (Fleck et al., 1994) and voluminous plutonism overprinted structural and sedimentologic features of the earlier extensional arc in many places. Furthermore, a recent paleogeographic reconstruction of the southern Inyo Mountains of eastern California suggests at least local uplift of the Jurassic arc (Dunne et al., 1998). Nonetheless, extensional or transtensional basins have been documented in relatively little deformed and only weakly metamorphosed domains along the length of the Jurassic arc in the Cordilleran United States

and Mexico (see previously cited references; also, Riggs and Busby-Spera, 1990; Fisher, 1990; Schermer and Busby, 1994; Wyld, 2000). South Cowhole Mountain (Fig. 1) is one of these domains.

In the late 1980s, we made a detailed map of the eastern half of the Cowhole Mountains at a scale of 1:5000, published for the first time here (Fig. 1). We restricted our field and petrographic studies to the eastern half of the range because silicic volcanic rocks datable by the U-Pb zircon method are interstratified with eolian quartz arenites there. In a 1989 abstract (Busby-Spera et al., 1989), as well as an informal guidebook article for a 1991 Penrose Conference field trip, we summarized evidence for extension during accumulation of the upper part of the section, and we reported dates indicating that the eolianites are age equivalent to the Middle Jurassic Temple Cap Sandstone or Carmel Formation, not the Lower Jurassic Navajo Sandstone. Subsequent mapping of the entire range by Wadsworth et al. (1995) supported our intra-arc extension model because they documented normal growth faults and landslide deposits in the lower part of the section. In this paper, we provide more detailed description and interpretation of the upper part of the section than given by Wadsworth et al. (1995). We describe the volcanologic and sedimentologic characteristics of the section, incorporating petrographic interpretation of ~100 thin sections. We also give map-scale and outcrop evidence, not recognized by other workers, for landsliding during normal faulting of the upper part of the section. Finally, we present and interpret our U-Pb zircon age data, which indicate a Middle Jurassic age for the section.

Although the Cowhole Mountains are only a “postage stamp” relative to the length of the Jurassic arc, the rocks there are particularly good for determining the age and paleogeographic setting of a segment of the Jurassic arc because (1) the sedimentary and volcanic strata are unusually well preserved and well exposed and (2) the numerous silicic volcanic units in the section allow us to check for geologic consistency in our U-Pb zircon age results. This check is important because U-Pb studies of continental metavolcanic rocks commonly suffer from zircon inheritance as well as Pb loss from the zircons, making their age interpretation difficult.

PREVIOUS WORK ON JURASSIC EOLIANITES IN THE EASTERN MOJAVE BLOCK

Hewett (1931) first applied the name “Aztec Sandstone” to eolian quartz arenite that overlies Triassic strata in the Spring Mountains of southwestern Nevada and correlated it with the Lower Jurassic Navajo Sandstone of the Colorado Plateau. He later extended this correlation to the Mescal Range in eastern California (Hewett, 1956), and this name and correlation have since been applied to the eolian quartz arenites in many other ranges of the Mojave block (Grose, 1959; Miller and Carr, 1978), including the Cowhole Mountains (Novitsky-Evans, 1978). Our age data presented here, however, indicate that at

least three-fourths and probably all of the Aztec Sandstone in the Cowhole Mountains is Middle Jurassic and thus younger than the Navajo Sandstone. In fact, subsequent studies of the Aztec Sandstone in the type locality, the Spring Mountains, as well as in the Mescal Range, show that age constraints remain too poor to determine whether the eolianites are Early, Middle, or Late Jurassic (Fleck et al., 1994). They could thus be correlative with the Glen Canyon Group, the San Rafael Group, or the Entrada Sandstone. There is only one well-dated Lower Jurassic eolianite in the Mojave block (Schermer et al., this volume), and other intra-arc eolianites previously assumed to be Navajo equivalents have yielded Middle Jurassic ages (e.g., southeast California, Fackler-Adams et al., 1997; southern Arizona, Riggs et al., 1993). To summarize, the name “Aztec Sandstone” has been applied to eolianites ranging from Early through Middle to possibly Late Jurassic age; thus that name no longer has any significance in terms of correlation with specific backarc eolianites of the present-day Colorado Plateau. Because so many previous workers have called the eolianites in the Cowhole Mountains “Aztec Sandstone,” we continue to do so (unit Ja, Figs. 1, 2, and 3). We emphasize, however, that “Aztec Sandstone” appears to span much of the Jurassic from locality to locality in the southwest Cordilleran United States.

Dunne (1972) and Novitsky-Evans (1978) termed the section of volcanic rocks that overlies the Aztec Sandstone in the Cowhole Mountains the “Delfonte Volcanics,” extending this name from the Mescal Range 25 km to the east. More recently, we dated the Delfonte Volcanics in the Mescal Range at 100.5 ± 2 Ma (Busby et al., 1994; Fleck et al., 1994). This is much younger than the preliminary age of 167 Ma we reported for the “Delfonte Volcanics” in the Cowhole Mountains (Busby-Spera et al., 1990b). For this reason, Wadsworth et al. (1995) renamed the volcanic rocks above the eolian sandstones the “Cowhole volcanics.” We follow this usage here (unit Jcv, Figs. 1, 2, and 3).

Marzolf (1980) reported that volcanic rocks not only overlie the Aztec Sandstone, but are interstratified with it at two stratigraphic levels, termed the upper volcanic unit and the lower volcanic unit. Wadsworth et al. (1995) referred to these as the lower and upper volcanic members of the Aztec Sandstone. We do not follow this subdivision because we interpret the “upper volcanic unit” (or “upper volcanic member”) as a sill, not a volcanic rock, as described subsequently. For this reason, we refer to the “lower volcanic unit” as “Aztec volcanics” (unit Jav, Figs. 1 and 2).

STRATIGRAPHY

Mesozoic strata in the Cowhole Mountains include up to 200–800 m of eolian quartz arenite overlain by more than 575 m of ignimbrites, lava flows, and minor sedimentary rocks (Fig. 2; Busby-Spera et al., 1990b; Wadsworth et al., 1995).

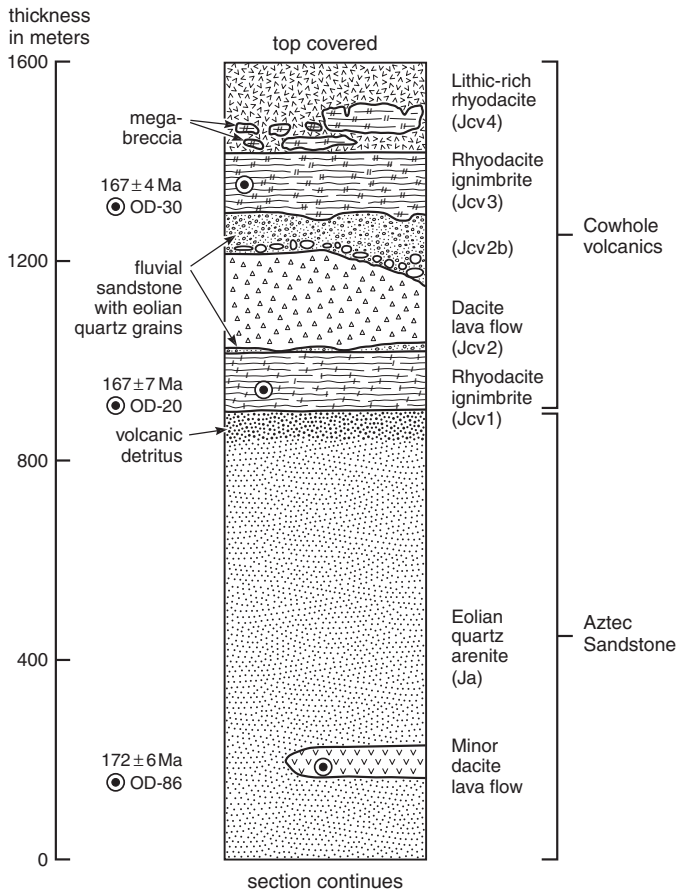


Figure 2. Composite stratigraphic column through Jurassic strata of the Cowhole Mountains. Thicknesses of most map units vary across area (see Fig. 1).

Aztec Sandstone

We agree with all previous workers in this area that the Aztec Sandstone in the Cowhole Mountains is predominantly an eolian quartz arenite (Novitsky-Evans, 1978; Marzolf, 1980; Wadsworth et al., 1995). It consists largely of stacked sets 1–10 m thick of tabular to trough cross-laminated, very well-sorted, medium-grained quartz sandstone, probably deposited on the foresets of eolian dunes. In thin section, it is a super-mature sandstone, consisting of >95% well-rounded mono-crystalline quartz grains. Along depositional contacts with some of the volcanic units, the quartz arenite is variably contaminated by volcanic lithic fragments, glass shards, and euhedral pyrogenic crystals. We refer the reader to the already-cited previous workers and others for more detailed sedimentologic descriptions of the Aztec Sandstone in the Cowhole Mountains that do not bear directly on the age and tectonic setting discussed in this paper.

Our study of the Aztec Sandstone has focused on igneous rocks within it for the purpose of (1) documenting the nature of any contemporaneous volcanism and (2) dating the Aztec

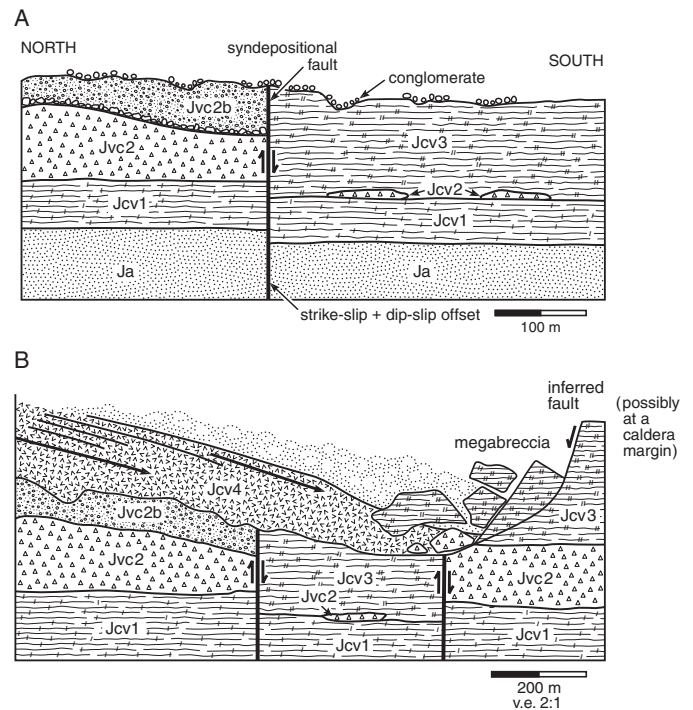


Figure 3. Cross-sectional reconstruction of syndepositional faulting and deposition of landslide megabreccias during accumulation of the Cowhole volcanics. (A) Syndepositional fault that bounds the southern margin of the uplifted block within the Aztec Sandstone and Cowhole volcanics (Fig. 1). The fault that bounds the northern margin of the uplifted block is incompletely exposed and is not portrayed here. The thickness of Cowhole volcanics unit 1 (Jcv1) does not change across the fault, although the fault clearly offsets its contact with the underlying Aztec Sandstone (Fig. 1). Changes in unit Jcv2 and Jcv2b across the fault could possibly indicate early syndepositional movements (see text). Strong evidence for syndepositional movement lies in the absence of unit Jcv3 on the upthrown block; this unit is an ignimbrite that elsewhere forms a laterally continuous sheet of even thickness (Fig. 1). We infer that uplift of this block resulted in erosional stripping of the ignimbrite (Jcv3) and deposition of a lag of boulder conglomerate composed of clasts of Jcv3 across the top of both blocks, overlapping the fault. (B) Deposition of lithic fragment-rich rhyodacite ignimbrite with megabreccia (Jcv4) across inactive syndepositional fault (left) during movement of inferred fault to the south of the present-day exposures (right). Like the underlying boulder conglomerate (Fig. 3A), the ignimbrite clearly overlies the syndepositional fault. The megabreccia wedge thickens and coarsens toward the inferred southern fault and is composed largely of clasts of the underlying two units (Jcv3 and Jcv2).

Sandstone by identifying interstratified silicic volcanic rocks suitable for U-Pb zircon dating.

Aztec volcanics. We mapped two lenses of volcanic rock within the Aztec Sandstone (unit Jav); one is at the north end of the map area, interpreted as a dacite lava flow (U-Pb zircon sample locality OD-86), and the other is near the south end of the map area, interpreted as a dacite tuff (Fig. 1). An igneous body in the upper part of the Aztec Sandstone at the north end of the map area has a more controversial origin. We interpret it

to be a felsic sill (Fig. 1), but Marzolf and Cole (1987) interpreted it to be a lava flow ("upper unit"), as did Wadsworth et al. (1995), who correlated it with the tuff described in this section. For that reason, we discuss the controversial igneous body in this section after describing the lava flow and the tuff.

The volcanic lens at the north end of the map area (unit Jav, Fig. 1) is interpreted as a lava flow because it is everywhere concordant with bedding in the Aztec Sandstone and has brecciated upper and lower margins, which would not be expected on the margins of sills. It is a crystal-rich lava flow, with ~40% plagioclase crystals, that is partially calcitized and epidotized. Wadsworth et al. (1995) interpreted this lava flow to be andesitic in composition (their "lower volcanic member"), but we suspect it is instead a dacite, because it yielded abundant zircon separates. Age data from this lava flow are presented subsequently.

The volcanic lens at the south end of the map area (unit Jav, Fig. 1) is a tuff that we interpret to represent a nonwelded ignimbrite (i.e., pumice-rich pyroclastic-flow deposit). It is a thick, nonstratified deposit, up to 25 m thick, composed of poorly sorted, noncompacted pumice lumps in a fine-grained matrix containing relict glass shards and lacking crystals. Its nonwelded character probably accounts for its highly altered and weathered condition relative to the thicker, more extensive welded ignimbrites of the overlying Cowhole volcanics (units Jcv1, Jcv3, Jcv4, Figs. 1 and 2). Because of this poor preservation, and because it is aphyric, we did not sample the nonwelded ignimbrite for U-Pb zircon geochronology. Wadsworth et al. (1995) correlated this volcanic lens with Marzolf and Cole's "upper unit" lava flow (which we infer is actually a sill), but that body bears phenocrysts, whereas the ignimbrite does not, so this correlation is not valid.

The igneous body that has been previously mapped as the upper volcanic unit (Marzolf and Cole, 1987) or upper volcanic member (Wadsworth et al., 1995) lies near the top of the Aztec Sandstone near its north end (to the southwest of zircon sample locality OD-20, Fig. 1). It is concordant with bedding, as a lava flow would be, but unlike most silicic lava flows, it is a perfectly tabular body with very sharp, nonbrecciated upper and lower contacts, and flow banding is best developed close to its margins. It also lacks the broken crystals or vitroclastic texture typical of tuffs, although pervasive perlitic fractures in the sill could be mistaken for vitroclastic texture. We therefore do not consider it a volcanic rock and thus did not sample it for dating of the section. The sill has large but sparse plagioclase, fewer potassium feldspar phenocrysts, and small sparse quartz phenocrysts; the rock is therefore probably a dacite. Similar greenish-tan flow-banded silicic sills and dikes cut the entire section in the Cowhole Mountains (Fig. 1).

Cowhole volcanics

We recognize four volcanic units within the Cowhole volcanics (Figs. 1 and 2). Unit 1 (Jcv1) is a rhyodacite ignimbrite

120 m thick, and unit 2 (Jcv2) is a dacite lava flow 200 m thick. Both units 1 and 2 are overlain by fluvial sandstones that contain a mixture of eolian quartz and pyroclastic debris, although the fluvial section above unit 2 is much thicker than the fluvial section above unit 1 (Fig. 2). For this reason, it is mapped separately from unit 2 and is referred to as unit 2b (Fig. 1). Unit 3 (Jcv3) is a rhyodacite ignimbrite. Unit 4 (Jcv4) is a lithic-rich rhyodacite ignimbrite, greater than 200 m, that contains a megabreccia with slabs up to 200 m thick derived from stratigraphically lower units. Its top is covered.

Unit 1 (Jcv1). The unit 1 ignimbrite is purplish red rhyodacite, with ~10% quartz, ~10% plagioclase, and ~5% potassium feldspar phenocrysts, plus sparse phenocrysts of a minor altered mafic mineral (probably hornblende). Quartz phenocrysts are large (up to 6 mm) and euhedral to embayed. The quartz and feldspar phenocrysts are commonly broken. The ignimbrite has eutaxitic texture owing to compaction of pumice. In thin section, the very well preserved matrix consists largely of sintered glass shards, indicating that the compaction fabric formed by welding in the hot state, rather than by diagenetic compaction. Volcanic lithic fragments are rare and include irregularly shaped, welded rhyolite tuff clasts. The uppermost 5–10 m of the unit 1 ignimbrite is nonwelded, with excellent preservation of nonsintered bubble-wall glass shards. Plagioclase phenocrysts are harder to recognize in the nonwelded top of the ignimbrite because they are more calcitized, probably owing to the greater permeability of the nonwelded top during diagenesis.

Fluvial sandstones overlie the nonwelded top of the unit 1 ignimbrite, but were not mapped separately because they are discontinuous and less than 2 m thick. They are thin- to medium-bedded, planar-laminated to ripple or trough cross-laminated sandstones and pebbly sandstones. The sandstones are tuffaceous, with euhedral volcanic quartz and feldspar grains and bubble-wall shards, probably derived at least in part from the underlying nonwelded top of the unit 1 ignimbrite. They contain silicic rock fragments, particularly in the coarse sand to pebble size fraction. The sandstones also contain a high proportion (25%–40%) of very well rounded, medium-sand-sized grains of monocrystalline quartz, identical to those in the Aztec Sandstone. Their presence indicates that eolian sand was still available after the eruption of unit 1 ignimbrite; the sand grains may have been supplied by active dunes or by reworking of nonlithified eolian deposits similar to those that lie beneath the unit 1 ignimbrite (Aztec Sandstone).

Unit 2 (Jcv2). Unit 2 is a dark purplish brown to dark gray dacite lava flow, with ~3% plagioclase and ~1% biotite phenocrysts, as well as rare altered mafic phenocrysts showing relict amphibole cleavage. The phenocrysts are set in a microcrystalline quartzofeldspathic mosaic with plagioclase microlites. The flow includes both coherent lava and much less common brecciated lava. The breccias occur at the base and top of the unit and have angular and closely packed clasts up to 30 cm long; these are interpreted to be autobreccias or "flow breccias." Flow

alignment of phenocrysts is best developed in the coherent (nonbrecciated) interior of the dacite lava flow. At some localities, the outer 1 m of the dacite lava flow locally shows relatively poorly vesiculated pumiceous texture and thick-walled bubble shards. These features indicate local development of a vesiculated (pumiceous) carapace on the lava flow. The restriction of flow breccia and pumiceous carapace to the bottom and top of unit 2 indicates that it represents a single lava flow. The basal contact of unit 2 is conformable with unit 1 in most of the map area, but in the north, it appears to cut across the upper part of unit 1 (Fig. 1). We interpret this discordant contact to represent a paleovalley cut into unit 1 and filled by unit 2. We do not think the contact is an intrusive contact, because the lava flow retains its basal-flow breccia and pumiceous carapace along this contact.

Unit 2b (Jcv2b). The sandstones above unit 2, unlike those above unit 1, are thick enough to map separately as unit 2b (Jcv2b, Fig. 1). Unit 2b is dominated by fluvial sandstones similar to those that lie at the top of unit 1, but debris-flow deposits are locally present at the base of unit 2b.

Fluvial sandstones of unit 2b consist largely of planar-laminated and ripple cross-laminated, thin-bedded, orangish-red sandstone, interbedded with maroon siltstone. These rocks are interstratified with medium-bedded, faintly laminated, pebbly sandstone and pebble conglomerate with angular volcanic lithic fragments, in beds that are generally planar-based but locally show scoured bases.

The debris-flow deposits that locally occur at the base of the unit are thick bedded to very thick bedded and have a poorly sorted pebbly sandstone matrix of the same composition as the well-sorted fluvial pebbly sandstones and pebble conglomerates. The debris-flow deposits lack internal stratification or clast alignment, are very poorly sorted, and contain angular clasts up to 1 m in length dispersed within the pebbly sandstone matrix. Blocks within the debris-flow deposits include the following (in order of abundance): unit 1 ignimbrite (Jcv1); unit 2 lava flow (Jcv2); sedimentary intraclasts; and basalt or andesite clasts of unknown provenance, some with plagioclase and an altered mafic mineral, others aphyric and vesicular. The basal few meters of unit 2b commonly contain abundant clasts of the unit 2 dacite flow-top breccia that were reworked into the overlying debris flows.

Like the fluvial sandstones above unit 1, the unit 2b sandstones, pebbly sandstones, and debris-flow deposits contain a significant (>25%) proportion of distinctive well-rounded to "dumbbell-shaped" eolian quartz grains. The ongoing availability of eolian quartz during deposition of the Cowhole volcanics is not surprising because their age is the same as that of the Aztec volcanics, within analytical error (discussed subsequently). The eolian quartz grains are mixed with angular volcanic quartz grains in subequal proportions and with much smaller quantities of silicic volcanic lithic clasts. Sparse feldspar, mica, and mafic volcanic clasts are also present.

Wadsworth et al. (1995) named the thick fluvial section

above the unit 2 dacite lava flow (our unit 2b) the "volcaniclastic unit (Jcv3)," but we believe this name obscures the fact that well-rounded quartz sand grains make up well over 25% of these sandstones.

Unit 3 (Jcv3). Unit 3 is a gray rhyodacite ignimbrite with ~5% euhedral, embayed, and broken quartz, ~5% plagioclase, and ~5% potassium feldspar phenocrysts in a matrix of sintered glass shards (welded tuff). The total crystal content of this ignimbrite is somewhat variable (~10%–20%), but the proportions of quartz, plagioclase, and potassium feldspar remain constant, and crystal content is lower than that of unit 1 ignimbrite. Preservation of the welded shards is not as good as that of the unit 1 ignimbrite, owing to microscopic quartzofeldspathic recrystallization that may represent vapor-phase devitrification. In some areas, recrystallization has destroyed vitroclastic texture, but broken crystals are abundant throughout the unit. Pumice lapilli are sparse, suggesting a higher fragmentation index during eruption of this pyroclastic flow relative to units 1 and 4. The greater proportion of broken versus nonbroken crystals in this unit relative to the other two ignimbrite units supports this hypothesis. Fiamme are more easily recognizable on weathered outcrops than they are on fresh outcrops or in thin section and are scattered throughout the unit.

Our unit 3 rhyodacite ignimbrite was mapped by Wadsworth et al. (1995) as a rhyolite intrusion (their Jr), even though they stated that the field evidence was "not completely compelling but permissive of an intrusive nature" (p. 337). We agree with Wadsworth et al. (1995) that the pyroclastic nature of the unit is more commonly evident in thin section (in the form of relict shards and broken crystals) than it is in outcrop (in the form of eutaxitic texture and fiamme). We do not agree with their interpretation of the unit as a very shallow level, vent-related intrusion with pyroclastic textures. We prefer the simpler interpretation that it is an ignimbrite, for several reasons. The tabular shape and concordance of unit 3 would require it to be a pyroclastic sill if it is intrusive. We are not aware of any pyroclastic sills reported in the literature, although vertical ignimbrite feeder dikes with steeply dipping welding compaction have been recognized by other workers (e.g., Reedman et al., 1987; Kano et al., 1997; Miura, 1999). The compaction foliation in unit 3 is bedding parallel. Furthermore, we recognize megablocks of unit 3 ignimbrite in the unit 4 lithic-rich ignimbrite. Wadsworth et al. (1995) mapped these megablocks as rhyolite intrusions (their Jr) into our unit 4. This interpretation is not possible, because the megablocks of unit 3 ignimbrite range continuously from decameters to decimeters in size. Additionally, cobbles of unit 3 ignimbrite form a conglomerate that locally underlies the unit 4 ignimbrite (described next). These relationships indicate that unit 3 was emplaced before emplacement of unit 4, so it cannot be an intrusion.

Unit 4 (Jcv4). Unit 4 is a brick red, lithic-rich rhyodacite ignimbrite with megabreccia (Figs. 1 and 2). It is nonwelded to weakly welded and consists of nonwelded to incipiently welded bubble-wall shards, pumice shreds, and broken crystals. It con-

tains up to 30% accidental lithic fragments, which may have helped to cool the ignimbrite below its welding temperature during emplacement. The unit 4 ignimbrite has a high crystal content similar to unit 1 (~30%), with subequal proportions of quartz, plagioclase feldspar, and potassium feldspar, and a few percent altered amphibole phenocrysts. Quartz phenocrysts are highly embayed. Lapilli-sized lithic fragments are all angular and include the following (in order of abundance): aphyric to porphyritic silicic volcanic clasts, limestone clasts, tuff clasts (with nonwelded bubble-wall shards), welded rhyolite tuff clasts, and clasts of fine-grained sandstone and siltstone.

Megablocks in the unit 4 ignimbrite are 1–200 m long and include the following (in order of abundance): unit 3 gray rhyodacite ignimbrite; unit 2 lava flow; unit 2b sedimentary rocks; and carbonate, especially toward the south end of the map area. Most megabreccia domains are dominated by very large megablocks, meters thick and tens of meters long, with lesser domains dominated by large megablocks several meters across. The largest megablocks are composed of unit 3 ignimbrite and are map scale in size (Fig. 1). Blocks of this size are found only in landslide deposits; the origin of these landslide megabreccias is discussed subsequently in a separate section.

Wadsworth et al. (1995) did not recognize the landslide blocks in the unit 4 ignimbrite, which they interpreted to be a rhyolite flow breccia with abundant lithic fragments derived from subjacent units. However, we know of no rhyolite lava flows choked with accidental fragments; furthermore, we recognize a matrix of pumice, shards, and broken crystals, indicating that unit 4 is a lithic-rich ignimbrite, not a lava flow. As noted previously, Wadsworth et al. (1995) mapped the large megablocks as intrusions, but these bodies consist of welded unit 3 ignimbrite with the orientation of pumice compaction fabrics varying from block to block, indicating that some of them tumbled. Lithic fragments become far less abundant high within the unit 4 ignimbrite (Figs. 1 and 2), and Wadsworth et al. recognized this part of the unit as an ignimbrite, dividing it off as a fifth unit; however, we consider it to be the same unit because it is in gradational contact and has identical minerals, microtextures, and field appearance (other than lower content of lithic fragments).

Rhyolite intrusions of uncertain age (fi). We discuss these under the Cowhole volcanics because they have been previously interpreted to be part of the Cowhole volcanics (Marzolf and Cole, 1987), although we reinterpret them here as shallow-level intrusions. Their alteration products are the same as those of the Cowhole volcanics (calcite plus epidote), suggesting that they may also be Jurassic, but they are not dated.

We mapped three felsic intrusions in the northern part of the map area (fi, Fig. 1): one that crosscuts the Aztec volcanics (Jav), a second that crosscuts the Aztec Sandstone (Ja) and unit 1 of the Cowhole volcanics (Jcv1), and a third that lies above unit 3 of the Cowhole volcanics (Jcv3) with a covered top (at the northeasternmost exposure on an isolated hill). These three we refer to as the lower, middle, and upper felsic intrusions,

respectively. All three felsic intrusions have sparse calcitized plagioclase phenocrysts in a felsitic groundmass (i.e., a microcrystalline mosaic of quartz and feldspar).

The middle felsic intrusion was informally referred to as “rhyolite ridge” by Marzolf and Cole (1987), who interpreted it as a lava flow filling a paleovalley in the Aztec Sandstone. We reinterpret “rhyolite ridge” as an intrusion rather than a lava flow because the body crosscuts vertically through bedding in the Aztec Sandstone and it has a pervasively well-developed flow banding that lies perfectly parallel to its vertical margins. It also lacks the flow breccias that lie along the bottoms and tops of nearly all rhyolite lava flows.

The upper felsic intrusion has not been previously mapped. We interpret this body as a sill, because its exposed lower contact and well-developed flow banding in the basal 1 m of the sill are concordant with local bedding and because it also lacks flow breccias. The sill has very well developed columnar jointing oriented perpendicular to local bedding. We speculate that the lower felsic intrusion may have been a feeder dike for this sill, although they are not connected in the cross-sectional view afforded by present-day exposures.

Summary of Cowhole volcanics. The Cowhole volcanics record the overwhelming of an eolian depositional environment (Aztec Sandstone) by proximal volcanic activity. This transition was probably gradual, as shown by the presence of silicic lava flows and ignimbrites in the upper part of the Aztec Sandstone that are similar to those of the overlying Cowhole volcanics. The abundance of eolian quartz sand grains in sedimentary units in the basal half of the Cowhole volcanics (Fig. 2) also supports the interpretation of a gradual transition from an eolian to a volcanic environment. The main evidence for proximal volcanic activity lies in the silicic lava flows of both the Aztec volcanics and the Cowhole volcanics, because nearly all silicic lava flows are too viscous to travel far from vents. The silicic lava flow in the Cowhole volcanics is much thicker than the silicic lava flow in the Aztec Sandstone, consistent with the interpretation that proximal volcanic activity (Cowhole volcanics) progressively overwhelmed eolian processes (Aztec Sandstone). U-Pb zircon dates on the Aztec volcanics and the Cowhole volcanics (presented later in this paper) support the interpretation that the two units are linked in time and basal setting.

Three out of the four units of the Cowhole volcanics are silicic ignimbrites over 100 m thick (Jcv1, Jcv3, and Jcv4, Fig. 2). These are likely the product of highly explosive eruptions at calderas. The top of the uppermost ignimbrite is covered, so its original thickness is not known, but the lower two are not thick enough to represent intracaldera accumulations. They are therefore interpreted as welded caldera outflow deposits. The uppermost unit, with its megabreccia, could possibly represent the fill of a small exposed sector of a much bigger, largely buried caldera (discussed further later in this paper).

Several features of the Cowhole volcanics suggest deposition within a tectonically active basin. First, episodic input of

large clasts from underlying units suggests that these units were quickly exposed in fault scarps. Unit 2b contains blocks derived from units 1 and 2; similarly, unit 4 contains blocks derived from units 2b and 3. Second, debris-flow deposits in unit 2b indicate local topographic relief. Third, fluvial deposits of the Cowhole volcanics are texturally and compositionally immature except for the eolian sand component; the fluvial deposits contain fewer traction structures than is typical of most such deposits, and they form aggradational sequences with little or no evidence of channelization. These characteristics suggest catastrophic sedimentation, which is typical of tectonically and volcanically active basins. In the following section, we describe two syndepositional faults within the map area, and we infer the existence of a third fault beyond the present limits of exposure.

SYNDEPOSITIONAL FAULTS AND LANDSLIDE MEGABRECCIAS

Our map shows two faults with roughly east-west trends that bound an uplifted block within the Cowhole volcanics and Aztec Sandstone (labeled with up and down symbols in Fig. 1). In this part of the paper, we provide evidence that this block was uplifted along normal faults after deposition of Cowhole volcanics unit 3 (Jcv3) and before deposition of Cowhole volcanics unit 4 (Jcv4). We discuss the southern fault boundary of the uplifted block first because the evidence for syndepositional movement on this fault is stronger. It is overlapped by unit 4 (Jcv4) of the Cowhole volcanics, so movement on it clearly predates deposition of that unit (Fig. 1). It is harder to prove that the northern fault set is syndepositional, because the relationship between it and the unit 4 ignimbrite, which presumably overlaps it, is not exposed (Fig. 1).

The subvertical fault on the southern boundary of the uplifted block separates strata of dramatically different thicknesses and lithologic characters. A cross-sectional reconstruction of this fault and the strata it cuts is presented in Figure 3A. The thickness of the unit 1 (Jcv1) ignimbrite does not change across the fault. The unit 2 (Jcv2) lava flow is considerably thinner and less continuous on the south side of the fault, relative to the north side, but silicic lava flows have very high aspect ratios with steep margins, so abrupt thinning of the lava flow cannot be used to prove syndepositional faulting. However, the sedimentary rocks above the unit 2 lava flow (unit Jcv2b) are restricted to the north side of the fault; this circumstance suggests that the fault may have had an early movement history that was down to the north, i.e., opposite in sense to its final movement (Fig. 3A). The most dramatic stratal change across the syndepositional fault is the abrupt disappearance of the unit 3 (Jcv3) ignimbrite, which is 125 m thick on the south side of the fault, but absent on the north side of the fault. Ignimbrites form sheet-like deposits that do not terminate abruptly, except against topographic barriers high enough to block the highly expanded, mobile flows that deposit them. We propose that the

unit 3 ignimbrite was originally deposited across the entire field area and then stripped off the uplifted block bounded by the southern and northern faults. The unit 3 ignimbrite reappears to the north of the uplifted block, where it is the same thickness (125 m) as it is to the south of the uplifted block.

The major fault on the northern boundary of the uplifted block dips 70°–80° to the north. It drops younger strata on its north side onto older strata on its south side and is thus mapped as a normal fault (Fig. 1). The other fault in the northern set (plus a small intervening fault) is subvertical, with minor displacement of uncertain sense. A minimum age of offset on the normal fault could be established by dating the felsic dike that crosscuts it (Fig. 1), but even if the age proved to be the same as the Cowhole volcanics, within analytical error, one could always argue that the fault is immediately postdepositional. We suggest that the reappearance of the 125-m-thick unit 3 ignimbrite in the area north of this fault provides more conclusive evidence that this fault is the same age as the syndepositional fault to the south (Fig. 1).

Erosional stripping of the entire 125 m of ignimbrite unit 3 (Jcv3) from the upthrown side of the southern fault resulted in deposition of a cobble to boulder lag deposit across the southern fault (Fig. 3A). The resulting conglomerate is composed entirely of clasts of the unit 3 welded ignimbrite. The conglomerate is too thin (only as much as 2 m thick) to map separately (Fig. 1), but it rests directly upon unit 3 ignimbrite south of the upthrown block and upon unit 2b sedimentary rocks north of the fault on the upthrown block (Fig. 3A). This stratigraphy indicates that the upthrown block was planed off by erosion prior to deposition of the unit 4 ignimbrite.

Just outside the map area, we infer the presence of a third fault having a listric geometry. Landslide blocks were shed along this inferred fault into the map area during eruption and emplacement of the unit 4 ignimbrite (Fig. 3B). Slide blocks are largest in the southernmost exposures of the unit 4 ignimbrite, and they are absent from the northern exposure of the unit 4 ignimbrite (Fig. 1), which is dominated by mesobreccias bearing clasts less than 1 m in diameter. The landslide megabreccia in the southern exposure of unit 4 has blocks up to 200 m long derived from Cowhole volcanics units 2 and 3, and at least one Paleozoic carbonate megablock at the southernmost end of the unit. We infer that the slide blocks were shed along a fault to the south beyond the limits of present-day exposures (Fig. 3B). This scarp exposed units 2 and 3, but apparently did not expose the unit 1 welded ignimbrite. The carbonate megablock in the south suggests that basement may also have been exposed, although this megablock could have been reworked from the Aztec Sandstone, which also contains carbonate megablocks that Wadsworth et al. (1995) inferred were shed from syndepositional normal faults. The Aztec Sandstone was probably not lithified enough to form slide blocks in the Cowhole volcanics at the time of their eruption.

The fact that the megabreccia is encased in ignimbrite suggests that it represents an intracaldera accumulation. If so, the

present-day exposures afford a view of only a small part of the floor of a presumably much larger buried caldera. The non-welded to weakly welded nature of the ignimbrite matrix, however, could be used to argue against an origin as an intracaldera accumulation, because intracaldera ignimbrites are commonly strongly welded. If the unit 4 ignimbrite is not a caldera fill, the catastrophic landslides may have been generated by seismicity along a fault outside the field area, similar to the syndepositional fault overlapped by the megabreccia within our field area. It seems unlikely, however, that this seismicity would precisely coincide with the emplacement of an outflow ignimbrite in the area; the poor welding could be explained by rapid cooling against the floor of the caldera, aided considerably by avalanching of cold rock fragments into the ignimbrite from a caldera wall. Thus it seems more likely that unit 4 represents an intracaldera megabreccia.

We speculate that the unit 4 caldera was sited along an extensional fault zone that we informally term “the Cowhole fault zone,” using our data and data from Wadsworth et al., (1995). We tentatively reinterpret the Cowhole thrust of Novitsky-Evans (1978), which lies immediately to the west of the area mapped in Figure 1, as a normal fault, because it puts younger Paleozoic carbonates on top of older Paleozoic carbonates and attenuates strata. That fault appears to be onlapped by part of the Aztec Sandstone, but ongoing normal faulting is indicated by fanning dips in the Aztec Sandstone–Cowhole volcanics section, abrupt stratal-thickness changes within the Aztec Sandstone, and the presence of carbonate-block breccias and megabreccias at two different stratigraphic levels within the Aztec Sandstone (Wadsworth et al., 1995). Our work shows that normal faulting continued through deposition of the Cowhole volcanics.

U-PB ZIRCON GEOCHRONOLOGY

Tera-Wasserburg plots for the three dated units from the Cowhole Mountains are in Figure 4, and data are presented in Table 1. All of the units show significant inheritance of older zircons. During the handpicking process, we separated frosted, rounded zircons, which we interpret to have been “entrained” during the passage of the ash flows over the ground surface. These entrained zircons (Fig. 4B) are not necessarily representative of the age of components inherited by the magma as it passed through the crust; inherited zircons, in contrast, serve as cores within the euhedral “igneous” zircons. Thus, our age interpretations are based heavily on data from the igneous zircons (Fig. 4A). For some of the fractions, we attempted to minimize common Pb and also the effects of possible later Pb loss by using step-wise dissolution techniques (e.g., Busby-Spera et al., 1990a; Mattinson, 1994). However, many of the samples still show some scatter about the regression lines. This scatter probably results from a range in ages of inherited components and/or from our inability to “see through” all of the effects of later Pb loss in the zircons. In addition, the data points for each

sample only show a moderate spread along the regression lines and are concentrated near the lower intercepts on concordia. These factors combine to produce moderately large uncertainties in the lower-intercept ages and very large uncertainties on the upper-intercept ages.

Regressions of the data for igneous-zircon fractions give the following intercept ages: Sample OD-86 (four igneous fractions) has a lower-intercept age of 172.4 ± 6.2 Ma and an upper-intercept age of 1334 ± 308 Ma. Sample OD-20 (four igneous fractions) has a lower-intercept age of 166.5 ± 6.7 Ma and an upper-intercept age of 764 ± 306 Ma. Sample OD-30 (three igneous zircons) has a lower-intercept age of 167.4 ± 3.5 Ma and an upper-intercept age of 1275 ± 302 Ma. The regressions thus all give lower intercepts that agree within errors at ca. 170 Ma. However, the argument could be made that the stratigraphically youngest sample, OD-30 (unit 3 of the Cowhole volcanics), is ~ 3 m.y. younger than a reference chord defined by the two stratigraphically older samples, OD-86 and OD-20 (shown in Fig. 4A). All three fractions for sample OD-30 lie clearly to the right (young side) of the reference chord. The upper-intercept ages for all three samples are very poorly determined, in part because of the long projection to the upper intercept with concordia. Nevertheless, they clearly indicate a Proterozoic inherited component.

A second concordia diagram (Fig. 4B) is shown with the same data but with the entrained, Precambrian fractions included. The entrained zircons seem generally older than the inherited fraction in the igneous zircons, although the upper intercept of the reference chord would just overlap within errors the apparently youngest entrained zircon point. This effect is a caution against using the ages of entrained zircons as a forced upper intercept for discordant igneous zircons.

Overall, our most robust conclusion is that the Aztec volcanics and the Cowhole volcanics all crystallized over a period of a few million years at ca. 170 Ma (Fig. 4A). The volcanics inherited zircons during the formation and evolution of their magmas and also entrained detrital zircons during their eruption and flow across the surface. The inherited and entrained zircons are Proterozoic, but span a range of ages; the inherited and entrained zircons do not necessarily represent the same population of zircons.

CONCLUSIONS AND REGIONAL CORRELATIONS

Intra-arc eolianites in the Cowhole Mountains, previously correlated with backarc eolianites of the Lower Jurassic Navajo Sandstone (Marzolf, 1980, 1990), are instead age equivalent to backarc eolianites of the Middle Jurassic Temple Cap and Carmel Formations dated by Kowalis et al. (2001). They are also age equivalent to intra-arc eolianites in the Palen Mountains of southeastern California (Fackler-Adams et al., 1997), as well as intra-arc eolianites of the upper member of the Mount Wrightson Formation and the strata of Cobre Ridge in southern Arizona (Riggs et al., 1993). These Middle Jurassic eolianites were

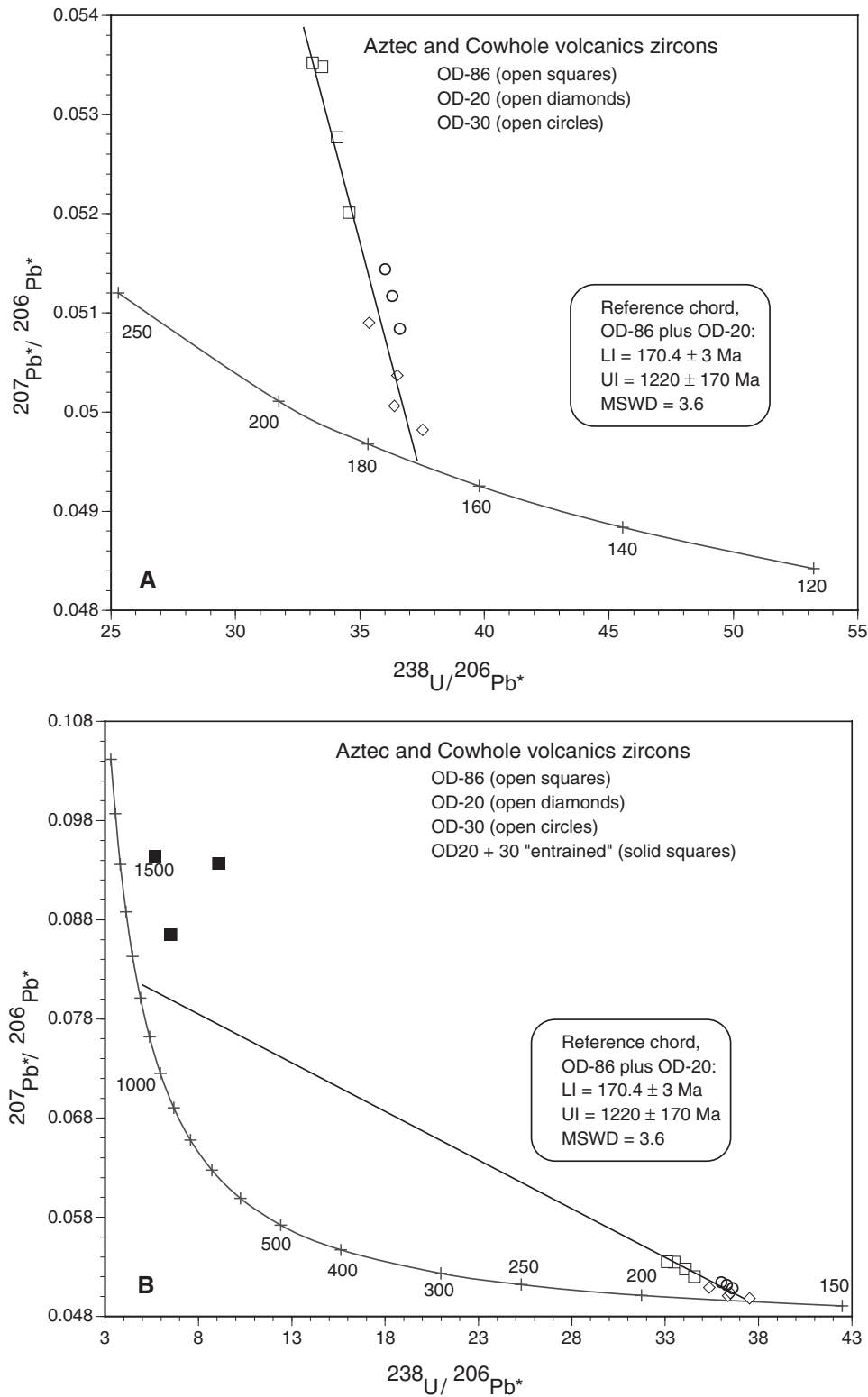


Figure 4. Tera-Wasserburg plots for U-Pb zircon data from the Aztec volcanics (OD-86) and the Cowhole volcanics (OD-20, from Cowhole volcanics unit 1, and OD-30, from Cowhole volcanics unit 3). Sample localities are presented in Figure 1 and stratigraphic relationships in Figure 2. (A) Regression of the data using igneous fractions only. (B) Concordia diagram shown with same data as Figure 4A plus inferred entrained Precambrian fractions. See text for interpretations. Abbreviations: LI—lower-intercept age, UI—upper-intercept age, MSWD—mean square of weighted deviates.

TABLE 1. ZIRCON DATA, COWHOLE MOUNTAINS

Sample [†]	Concentrations (ppm)			Isotopic ratios [§]	
	²⁰⁶ Pb*	²³⁸ U	²⁰⁴ Pb/ ²⁰⁶ Pb	²³⁸ U/ ²⁰⁶ Pb*	²⁰⁷ Pb*/ ²⁰⁶ Pb*
OD-86 100–151	3.858	147.5	0.000214	33.102 (191.9 ± 1.9)	0.05352 (351 ± 4)
OD-86 151–206	5.976	231.1	0.000109	33.473 (189.7 ± 1.9)	0.05348 (349 ± 2)
OD-86 206–320A	6.988	275.1	0.000074	34.087 (186.4 ± 1.9)	0.05277 (319 ± 2)
OD-86 206–320B	7.844	313.1	0.000051	34.566 (183.8 ± 1.8)	0.05201 (286 ± 2)
OD-20 100–200	10.005	408.6	0.000122	35.361 (179.7 ± 1.8)	0.05090 (236 ± 6)
OD-20 100–200	5.592	235.7	0.000541	36.496 (174.3 ± 1.7)	0.05037 (212 ± 5)
OD-20 <200	9.398	394.8	0.000128	36.377 (174.8 ± 1.7)	0.05006 (198 ± 6)
OD-20 <200	8.254	357.8	0.000355	37.523 (169.6 ± 1.7)	0.04982 (187 ± 4)
OD-20 100–200pC	13.391	140.6	0.000074	9.088 (673 ± 7)	0.09368 (1502 ± 2)
OD-30 100–200	5.488	228.3	0.000245	36.010 (176.5 ± 1.8)	0.05144 (260 ± 5)
OD-30 <200	7.535	315.9	0.000161	36.298 (175.1 ± 1.8)	0.05117 (248 ± 10)
OD-30 <200	5.626	237.9	0.000218	36.603 (173.8 ± 1.7)	0.05084 (234 ± 3)
OD-30 100–200pC	23.031	150.9	0.000047	5.670 (1047 ± 10)	0.09440 (1516 ± 2)
OD-30 <200pC	22.242	167.1	0.000069	6.504 (922 ± 9)	0.08649 (1349 ± 3)

*Radiogenic.

[†]“pC” designates frosted, rounded “entrained zircon fraction”. Numbers refer to grain size range in micrometers[§] ²⁰⁴Pb/²⁰⁶Pb ratio = measured, corrected for amount of ²⁰⁴Pb in spike. Calculated isotopic ratios for Terra-Wasserburg concordia diagram shown with calculated ages and uncertainties shown in parentheses. We have assigned a conservative 1% error to the ²³⁸U/²⁰⁶Pb* ratios to account for any minor fractionations during the step-wise dissolution procedure. For other analytical details, see Mattinson (1994).

also previously correlated with the Lower Jurassic Navajo Sandstone (Drewes, 1971; Bilodeau and Keith, 1986; Marzolf, 1990). Other intra-arc eolianites in Arizona and California, however, are age-equivalent to the Lower Jurassic Navajo and Wingate Sandstones (see discussion in Riggs et al., 1993). Craton-derived eolian sand was therefore trapped within intra-arc rift basins for a protracted period of time (at least 40 m.y.), not just during deposition of the Lower Jurassic Navajo Sandstone. Our Middle Jurassic dates from the Cowhole Mountains provide further evidence for this regional-scale interpretation.

We have previously obtained ages on volcanic rocks from the central and southeastern Mojave block that are similar to the ages from the eastern Mojave block reported here. Outflow ignimbrites of the Cowhole volcanics (Jcv1 and Jcv3), as well as the dacite lava flow within the Aztec Sandstone, are age equivalent to two of the intracaldera ignimbrites of the lower Sidewinder Volcanic Series of the central Mojave block, described by Schermer and Busby (1994) and Schermer et al. (this volume). The ignimbrites of the Cowhole volcanics are younger than the oldest lower Sidewinder ignimbrite and older than the youngest lower Sidewinder ignimbrite (Schermer et al., this volume). The ages of the Aztec volcanics and the Cowhole volcanics in the Cowhole Mountains also overlap with the basal Dome Rock volcanic sequence in the Palen Mountains. There we dated a silicic block-and-ash-flow deposit within a volcaniclastic unit that interfingers with underlying eolian quartz arenites, at 174 ± 8 Ma (Fackler-Adams et al., 1997). Our date on the top of the Dome Rock sequence, which interfingers with the basal McCoy Mountains Formation, is younger than the Cowhole volcanics, with an age of 162 ± 3 Ma on an ignimbrite (Fackler-Adams et al., 1997).

Our structural data from the upper half of the Cowhole

Mountains section, together with the data of Wadsworth et al. (1995) from the lower half of the section, indicate extension throughout deposition of the section there. Syndepositional normal faulting and deposition of landslide megabreccias accompanied Middle Jurassic eolian sedimentation and volcanism in the Cowhole Mountains (Wadsworth et al., 1995, and this study). Our volcanologic data show that silicic welded tuffs are the predominant volcanic rock type in the Cowhole Mountains, suggesting the presence of nearby calderas, and the youngest ignimbrite may represent an intracaldera accumulation.

Our previous studies in Middle Jurassic rocks of southern Arizona, southeastern California, eastern California, and the central Mojave block document ignimbrite eruptions from calderas contemporaneous with deposition of craton-derived eolian sands within the arc, in transtensional or extensional basins (Riggs and Busby-Spera, 1991; Schermer and Busby, 1994; Fackler-Adams et al., 1997). Silicic calderas are best developed in arcs undergoing extension or transtension, be they continental (e.g., Central America; North Island, New Zealand; Sumatra) or oceanic (e.g., Izu-Bonin). Extensional or transtensional arcs are also low-standing enough to act as a depocenter for sediment derived from outside of the arc, rather than acting as a high-standing topographic barrier the way neutral or compressional arcs commonly do. We suggest that extensional or transtensional basins within the Middle Jurassic arc of Arizona and southern California acted as efficient “traps” for eolian sands derived from the North American craton.

ACKNOWLEDGMENTS

This work was begun when C. Busby was a Ph.D. student (1978–1982), supported by Princeton University’s Department

of Geological Sciences and a National Science Foundation (NSF) dissertation fellowship. She thanks Princeton and, in particular, John Suppe and Franklyn Van Houten for their very generous financial and intellectual support throughout her graduate career. She thanks the editor of this volume, Allen Glazner, for encouraging her to pursue studies in the Mojave Desert when she bumped into him in the field there in 1979. Continued support for this study was provided by NSF grants EAR-8519124 and EAR-8803769 (to Busby and Mattinson). We are most grateful to John Marzolf and Doug Walker for field discussions in the Cowhole Mountains. Formal reviews by George Dunne and an anonymous reviewer helped to improve the manuscript substantially.

REFERENCES CITED

- Bilodeau, W.L., and Keith, S.B., 1986, Lower Jurassic Navajo-Aztec-equivalent sandstones in southern Arizona and their paleogeographic significance: *American Association of Petroleum Geologists Bulletin*, v. 70, p. 690–701.
- Busby, C.J., Mattinson, J.M., Parris, M., and Fackler-Adams, B., 1994, Timing and nature of late Mesozoic deformational events in southeastern California: Stratigraphic and geochronologic constraints: *Boulder, Colorado, Geological Society of America Abstracts with Programs*, v. 26, no. 2, p. 42.
- Busby-Spera, C.J., 1988, Speculative tectonic model for the early Mesozoic arc of the southwest Cordilleran United States: *Geology*, v. 16, p. 1121–1125.
- Busby-Spera, C.J., Schermer, E.R. and Mattinson, J.M., 1989, Volcano-tectonic controls on sedimentation in an extensional continental arc: A Jurassic example from the eastern Mojave Desert, California: Socorro, New Mexico, New Mexico Bureau of Mines and Mineral Resources Bulletin 131, p. 34.
- Busby-Spera, C.J., Mattinson, J.M., Riggs, N.R., and Schermer, E.R., 1990a, The Triassic-Jurassic magmatic arc in the Mojave-Sonoran deserts and the Sierran-Klamath region: Similarities and differences in paleogeographic evolution, in Harwood, D., and Miller, M.M., eds., *Paleozoic and early Mesozoic paleogeographic relations, Sierra Nevada, Klamath Mountains, and related terranes*: Geological Society of America Special Paper 255, p. 325–338.
- Busby-Spera, C.J., Mattinson, J.M., and Schermer, E.R., 1990b, Stratigraphic and tectonic evolution of the Jurassic arc: New field and U-Pb zircon geochronological data from the Mojave Desert: *Geological Society of America Abstracts with Programs*, v. 22, no. 3, p. 11–12.
- Drewes, H., 1971, Mesozoic stratigraphy of the Santa Rita Mountains, southeast of Tucson, Arizona: U.S. Geological Survey Professional Paper 748, 35 p.
- Dunne, G.C., 1972, *Geology of the Devil's Playground area, eastern Mojave Desert, California* [Ph.D. thesis]: Houston, Texas, Rice University, 79 p.
- Dunne, G.C., Garvey, T.P., Osborne, M., Schneider, D., Fritsche, A.E., and Walker, J.D., 1998, Geology of the Inyo Mountains volcanic complex: Implications for Jurassic paleogeography of the Sierran magmatic arc in eastern California: *Geological Society of America Bulletin*, v. 110, p. 1376–1397.
- Fackler-Adams, B.N., Busby, C.J. and Mattinson, J.M., 1997, Jurassic magmatism and sedimentation in the Palen Mountains, southeastern California: Implications for regional tectonic controls on the Mesozoic magmatic arc: *Geological Society of America Bulletin*, v. 109, p. 1464–1484.
- Fisher, G.R., 1990, Middle Jurassic syntectonic conglomerate in the Mount Tallac roof pendant, northern Sierra Nevada, California: *Geological Society of America Special Paper* 255, p. 339–350.
- Fleck, R.J., Mattinson, J.M., Busby, C.J., Carr, M.D., Davis, G.A., and Burchfiel, B.C., 1994, Isotopic complexities and the age of the Delfonte volcanic rocks, eastern Mescal Range, southeastern California: Stratigraphic and tectonic implications: *Geological Society of America Bulletin*, v. 106, p. 1254–1266.
- Grose, L.T., 1959, Structure and petrology of the northeast part of the Soda Mountains, San Bernardino County, California and southwestern Arizona: *Geological Society of America Bulletin*, v. 70, p. 1509–1548.
- Hewett, D.F., 1931, Geology and ore deposits of the Goodsprings quadrangle, Nevada: U.S. Geological Survey Professional Paper 162, 162 p.
- Hewett, D.F., 1956, Geology and mineral resources of the Ivanpah quadrangle, California and Nevada: U.S. Geological Survey Professional Paper 275, 172 p.
- Kano, K.J., Matsuura, H., and Yamauchi, S., 1997, Miocene rhyolitic welded tuff infilling a funnel-shaped eruption conduit, Shiotani, southeast of Matsue, SW Japan: *Bulletin of Volcanology*, v. 59, p. 125–135.
- Kowalis, B.J., Christiansen, E.H., Deino, A.L., Zhang, C., and Everett, B., 2001, The record of Middle Jurassic volcanism in the Carmel and Temple Cap Formations of southwestern Utah: *Geological Society of America Bulletin*, v. 113, p. 373–387.
- Marzolf, J.E., 1980, The Aztec sandstone and stratigraphically related rocks in the Mojave Desert, in Fife, D.L., and Brown, G.R., eds., *Geology and mineral wealth of the California desert*: Santa Ana, California, South Coast Geological Society, p. 215–220.
- Marzolf, J.E., 1990, Reconstruction of extensionally dismembered early Mesozoic sedimentary basins, southwestern Colorado Plateau to the eastern Mojave Desert, in Wiernicke, B.P., ed., *Basin and range extensional tectonics near the latitude of Las Vegas, Nevada*: Geological Society America Memoir 176, p. 477–500.
- Marzolf, J.E., and Cole, R.D., 1987, Relationship of the Jurassic volcanic arc to backarc stratigraphy, Cowhole Mountains, San Bernardino County, California, in Hill, M.L., ed., *Geological Society of America Centennial Field Guide*, v. 1, p. 115–120.
- Mattinson, J.M., 1994, A study of complex discordance in zircons using stepwise dissolution techniques: *Contributions to Mineralogy and Petrology*, v. 116, p. 117–129.
- Miller, E.L., and Carr, M.D., 1978, Recognition of possible Aztec-equivalent sandstones and associated Mesozoic metasedimentary deposits within the Mesozoic magmatic arc in the southwestern Mojave Desert, in Howell, D.G., ed., *Paleogeography of the western United States: Pacific Section, Society of Economic Paleontologists and Mineralogists, Pacific Coast Paleogeography Symposium*, p. 283–289.
- Miura, D., 1999, Arcuate pyroclastic conduits, ring faults, and coherent floor at Kumano caldera, southwest Honshu, Japan: *Journal of Volcanology and Geothermal Research*, v. 92, p. 271–294.
- Novitsky-Evans, J.M., 1978, *Geology of the Cowhole Mountains, southern California*: Structural, stratigraphic and geochemical studies [Ph.D. thesis]: Houston, Texas, Rice University, 95 p.
- Reedman, A.J., Park, K.H., Merriman, R.J., and Kim, S.E., 1987, Welded tuff infilling a volcanic conduit at Weolseong, Republic of Korea: *Bulletin of Volcanology*, v. 49, p. 541–546.
- Riggs, N.R., and Busby-Spera, C.J., 1990, Evolution of a multi-vent volcanic complex within a subsiding arc graben depression: Mount Wrightson Formation, Arizona: *Geological Society of America Bulletin*, v. 102, p. 1114–1135.
- Riggs, N.R., and Busby-Spera, C.J., 1991, Facies analysis of an ancient, dismembered, large caldera complex and implications for intra-arc subsidence: Middle Jurassic strata of Cobre Ridge, southern Arizona, U.S.A.: *Sedimentary Geology*, v. 74, p. 39–68.
- Riggs, N.R., Mattinson, J.M., and Busby, C.J., 1993, Correlation of Mesozoic eolian strata between the magmatic and the Colorado Plateau: New U-Pb

- geochronologic data from southern Arizona: Geological Society of America Bulletin, v. 105, p. 1231–1246.
- Schermer, E.R., and Busby, C.J., 1994, Jurassic magmatism in the central Mojave Desert: implications for arc paleogeography and preservation of continental volcanic sequences: Geological Society of America Bulletin, v. 106, p. 767–790.
- Wadsworth, W.B., Ferriz, H., and Rhodes, D.D., 1995, Structural and stratigraphic development of the Middle Jurassic magmatic arc in the Cowhole Mountains, central-eastern Mojave Desert, California, *in* Miller, D.M., and Busby, C., eds., Jurassic magmatism and tectonics of the North American Cordillera: Geological Society of America Special Paper 299, p. 327–349.
- Wyld, S.J., 2000, Triassic evolution of the arc and back-arc of northwest Nevada, and evidence for extensional tectonism, *in* Gehrels, G.E., ed., Paleozoic and Triassic paleogeography and tectonics of western Nevada and northern California: Geological Society of America Special Paper 347, p. 185–207.

MANUSCRIPT ACCEPTED BY THE SOCIETY MAY 9, 2001

